

# Frequency Inverter with Optimized Harmonics Distortion

LUIS DAVID PABON, EDISON ANDRES CAICEDO, JORGE LUIS DIAZ RODRIGUEZ,  
ALDO PARDO GARCIA.

Department of Electrical Engineering and Mechatronics  
University of Pamplona  
Ciudadela Universitaria, Km 1 via Bucaramanga, Pamplona  
COLOMBIA

[davidpabon@unipamplona.edu.co](mailto:davidpabon@unipamplona.edu.co), [acaicedo@hotmail.com](mailto:acaicedo@hotmail.com), [jdiazcu@unipamplona.edu.co](mailto:jdiazcu@unipamplona.edu.co) ,  
[apardo13@unipamplona.edu.co](mailto:apardo13@unipamplona.edu.co)

*Abstract-* The present paper shows the development of a frequency inverter by means of a common source three-phase multilevel inverter of 15 steps, this adopts modulations found by means of a multiobjective optimization algorithm, developed in Matlab, which allows obtaining a law of voltage vs. frequency that reduces the value of the voltage as the frequency decreases maintaining the total of harmonic distortion (evaluated until the harmonic 50 at levels very close to 0%, in the entire range of operating frequencies. The control of the inverter is done by FPGA Virtex5. The experimental tests shown in the work allow to validate the THD optimization in the whole frequency range and the good behavior of the common source multilevel inverter as a frequency inverter.

*Key-Words:* - Harmonics, multilevel inverter, PWM, FPGA, optimization, genetic algorithm.

## 1. Introduction

The power converters DC/AC, AC/AC and DC/DC are very used elements in the current industry, one example of this are the frequency inverters, applied in the speed control of asynchronous machines [1]; these inverters when changing the frequency of the motor supply change the synchronous speed and therefore the mechanical speed of the motor. This process is carried out by obtaining voltages of variable frequency and magnitude [2], whose actuation law will depend on the requirements of the control technique to be used [3].

A well-known principle in the speed control of speed of electrical machines is the law of scalar control "V vs f", this establishes that in order not to saturate the machines, the supply real mean square (RMS) voltage must decrease as the frequency falls from its rated value [4], usually to make this change of effective voltages and frequency, conventional inverters using pulse width modulations (PWM) are used. These modulations vary the frequency and voltage level by controlling the duration of the pulses within the waveform and the period of the same [1].

These inverters present problems in terms of power quality [5], because their output voltage has a not sinusoidal waveform, which causes a high harmonic content [6], [7], which can cause heating of the windings

and generation of opposite parasitic torque in the induction machine [7], [5]. Since the voltage waveform will depend on the voltage level required and the frequency, the THD of the drive changes as the frequency and the effective value of the voltage varies, becoming a function of the RMS value and the switching frequencies THD ( $V_{rms}$ , f) [8].

In order to solve this problem of harmonic distortion in DC / AC conversion of inverters and inverters in general, multilevel power inverters have appeared as a very good alternative [9], [10]. Presenting multiple works in the area of the optimization of the harmonic content of the inverters at constant frequency [11] - [16] and some approximations in the application [17] - [19] and the optimization in the area of the variable frequency in the control of electric machines [15], [20], [21]. Ratifying the benefits that multilevel investors have as electric machine feeders [22], [23].

This is why this article presents the implementation of a multilevel frequency inverter of 9 steps per phase and line 15, which has a low THD and independent of the RMS voltage level and the desired frequency, that is, an optimized THD in the entire range of operating frequencies. Likewise, it uses the multilevel inverter topology of common source H bridges, which according

to some works is reported as not recommended for variable frequency applications due to the saturation of the transformers [24] [31], however in this work to the use of a design methodology proposed by the authors, it is evident that the inverter can be used in these applications [25].

### 2. Multi-Level Inverter With Nine Steps Per Phase and 15 Line Steps

The multilevel inverter topology selected for this work is the common source asymmetric cascade H bridge inverter with a 2-stage 1: 3 ratio, which generates 9 voltage levels at the output of each phase, the potential difference of the phase voltages generates a line voltage with 15 steps, this topology is shown in figure 1 [11].

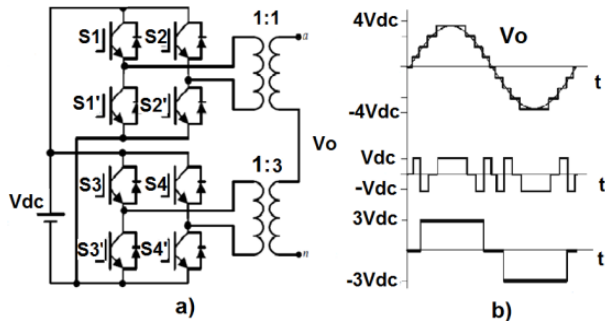


Fig. 1. Cascade asymmetric inverter common source of two stage with 9 levels at the out voltage, asymmetry 1:3  
a) topology. b) Output voltage.

In the Figure 2 shows the three-phase topology that is not more than the triplicate of the phase presented in figure 1, as you can see the three phases share the DC bus [14].

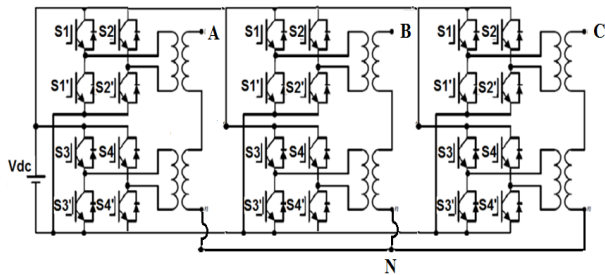


Fig. 2. Inverter topology.

### 3. Mathematical Modelling

In order to obtain an algorithm that allows to vary the frequency and voltage, maintaining a very low value of harmonic distortion, it was necessary to obtain equations that quantify the RMS value and the THD of the line voltage wave, in terms of the shooting angles per phase; For this, the Fourier series of the phase voltages were

determined and the series of the line voltage was calculated as the difference of the phase series, as shown in equation:

$$v_{AB}(t) = v_B(t) - v_A(t)$$

In this way, with the Fourier series of the line voltage, the RMS value and the THD in terms of the harmonics are quantified. In Figure 3 shows the first quarter waveform of phase A of a three-phase system of nine steps per phase [11]

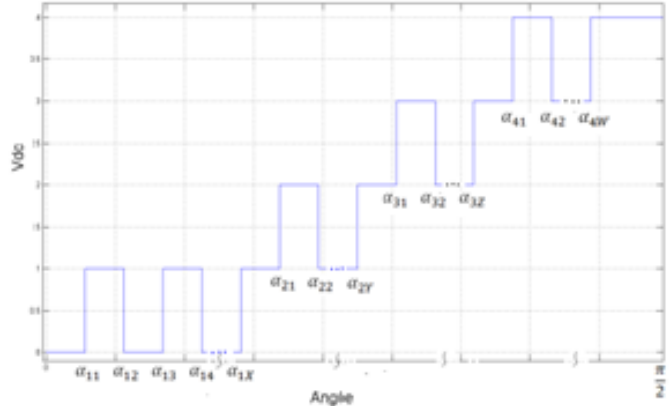


Fig.3. The ¼ waveform of the modulation in terms of on and off angles of each step.

As the form of the modulation shown saves 1/4 wave symmetry, it is only necessary to define the firing angles in the first quarter wave, the other parts of the phase modulation and the other two phases are constructed by trigonometric ratios. In this way we define a vector  $L = [a \ b \ c \ d]$  that represents the total number of on and off angles in each step. The Fourier series for periodic waveforms states:

$$v(t) = \frac{a_0}{2} + \sum_{n=1}^{\alpha} h_n * sen(wt + \varphi_n) \tag{1}$$

Where,  $h_n$  is the peak magnitude of the harmonic  $n$  and  $\varphi_n$  their respective phase shift, which are defined as:

$$h_n = \sqrt{a_n^2 + b_n^2} \tag{2}$$

$$\varphi_n = \tan^{-1} \frac{a_n}{b_n} \tag{3}$$

The Fourier series for the waveform of Phase A is defined by:

$$h_n = \begin{cases} 0 & \text{for } n \text{ pair} \\ \frac{4v_{dc}}{\pi n} \sum_{i=1}^4 \sum_{j=1}^{L_i} (-1)^{j-1} \cos n \alpha_{ij} & \text{for } n \text{ odd} \end{cases} \tag{4}$$

$$\varphi_n = 0 \tag{5}$$

Where  $V_{dc}$  is the voltage value of each step, and  $\alpha_{ij}$  is the angle  $j$  of the step  $i$ .

For phase B, which is displaced 120° electrical with respect to phase A, the Fourier series will be defined by:

$$h_n = \begin{cases} 0 & \text{for } n \text{ pair} \\ \frac{4vdc}{\pi n} \left( \sum_{i=1}^4 \sum_{j=1}^{L_i} (-1)^{j-1} \cos n \alpha_{ij} \right) & n \text{ odd non mult of } 3 \end{cases} \quad (6)$$

$$\varphi_n = \begin{cases} - & \text{for } n \text{ pair} \\ 0 & \text{for } n \text{ odd non multiple of three} \\ \frac{2\pi}{3} (-1)^{k+1} & \text{for } n \text{ odd non multiple of three} \end{cases} \quad (7)$$

Where, k is the appearance of the odd harmonic does non multiple of three, ie k = 1, for the harmonic 5, k = 2, for the harmonic 7, k = 3, for the harmonic 11, so on Making the respective differences in terms of the Fourier series of Phases A and B, we obtain the Fourier series for the line voltage V<sub>AB</sub>, of which in the article only the amplitude of the harmonics in the equation is presented (8), since the objective is to minimize the THD and calculate the RMS value, for this the phase shifts are not required:

$$h_n = \begin{cases} 0 & \text{for } n \text{ pair} \\ 0 & \text{for } n \text{ odd non mult of } 3 \\ \frac{4\sqrt{3} Vdc}{\pi n} \left[ \sum_{i=1}^4 \sum_{j=1}^{L_i} (-1)^{j-1} \cos n \alpha_{ij} \right] & \text{for } n \text{ odd non mult of } 3 \end{cases} \quad (8)$$

THD of line voltage

The IEEE 519 of 1992 defines the total harmonic distortion as (9) [29]:

$$THD = \frac{\sqrt{\sum_{n=2}^{50} h_n^2}}{h_1} \cdot 100 \quad (9)$$

Where the harmonic h<sub>1</sub> is the fundamental component and h<sub>n</sub> the peak of the harmonic n. Replacing (8) in (9):

$$THD = \frac{\sqrt{\sum_{n=2}^{50} \left( \frac{1}{n} \left[ \sum_{i=1}^4 \sum_{j=1}^{L_i} (-1)^{j-1} \cos n \alpha_{ij} \right]^2 \right)}}{\left[ \sum_{i=1}^4 \sum_{j=1}^{L_i} (-1)^{j-1} \cos 1 \alpha_{ij} \right] \cdot 100} \quad (10)$$

Where n takes odd values do non multiple of three, that is to say 5, 7, 11, 13, 17, ... td, and L<sub>i</sub> are the components of the vector L = [a b c d].

In the same way, the effective value can be defined in terms of harmonics such as:

$$V_{line_{RMS}} = \sqrt{\sum_{n=1}^{\alpha} V_{rms_n}^2} \quad (11)$$

Replacing an upper bound h<sub>max</sub> = 50 the V<sub>rms</sub> is determined by the equation (12)

$$V_{line_{RMS}} = \sqrt{\sum_{n=1}^{50} \left( \frac{4\sqrt{3} Vdc}{\pi n} \left[ \sum_{i=1}^4 \sum_{j=1}^{L_i} (-1)^{j-1} \cos n \alpha_{ij} \right] \right)^2} \quad \text{for } n = 5, 7, \dots \text{ odd non mult of } 3 \quad (12)$$

In this way in (10) the THD equation is defined as the objective function to be minimized by the optimization algorithm and in (12) the restriction equation, in this way the algorithm will look for a modulation with a certain RMS value and with the minimum THD, the frequency will depend on the implementation times, so the inverter can reproduce modulations with a certain frequency, voltage level and minimum harmonic distortion

### Scalar Law V/Hz

In order to avoid the saturation of the machines that the frequency inverter feeds, the voltage must be decreased as the frequency decreases from its rated value [1], this decrease is proportional to the reduction of the frequency, and in this work this law takes the form of the function of equation (13):

$$V(f) = \begin{cases} \left( \frac{V_n}{f_n - f_i} \right) (f - f_i) + V_{boost} & \text{for } f < f_{nom} \\ V_n & \text{for } f \geq f_{nom} \end{cases} \quad (13)$$

Where V<sub>n</sub> and f<sub>n</sub> are the rated voltage and rated frequency of the machine, f<sub>i</sub>, the initial frequency of the operating frequency range, V<sub>boost</sub>, the RMS level of the voltage at the initial frequency and f the desired frequency at the output of the inverter.

### Optimization algorithm

To develop the optimization of the modulations throughout the frequency range, genetic algorithms [28] [30] were used as an optimization technique, in order to make equation 10 as close as possible to zero and equation 12 approach to a greater extent a voltage value given by the scalar law; in this way the authors propose the algorithm shown in figure 4 to solve the optimization problem.

In the algorithm as the first measurement the rated values of the machine are assigned, these are line voltage (V<sub>n</sub>) and rated frequency (f<sub>n</sub>), the range of frequencies on which the control law is going to be entered (f<sub>i</sub>, f<sub>f</sub>) and the frequency step with which the voltage-frequency relation (Δf) is to be calculated. Then the user is given the maximum number of generations with which the multi-objective genetic algorithm (N<sub>max</sub>) should operate in each modulation. With these data the algorithm calculates a vector of frequencies and a vector of RMS voltage according to a law that is designated as a mathematical equation V<sub>(f)</sub>, for the case of this work the selected law is

the one shown in equation 13. With this for each frequency, the algorithm calculates a modulation with the respective RMS value and optimum THD.

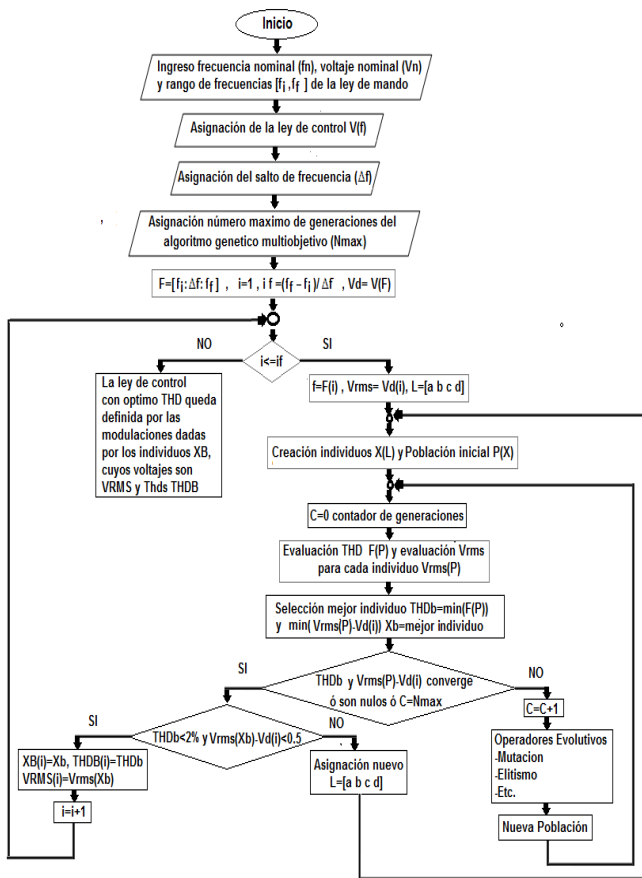


Fig. 4. Genetic algorithm multi objective optimization on the command law V/Hz

With the help of the Matlab® and the *gamultiobj* command, the algorithms corresponding to the mathematical model of the fitness functions (Equations 10 and 12) and their respective optimization by means of multiobjective genetic algorithms were programmed.

### 4. Optimization Algorithm Results

The rated voltage of the machine is assigned at 220 Vrms, the rated frequency 50 Hz, The frequency range of [1 Hz, 100 Hz] with steps of  $\Delta f = 0.5$  Hz, the  $V_{boost}$  level is set to 30 Vrms of line. With these data, the activation angles of 200 modulations with optimum harmonic content and with RMS values that follow the law V vs f given by equation 13 with the previous data were obtained. Table 1 shows a fragment of this information.

Table 1. Optimization

f	k	a	b	c	d	TC	VRMS	THD	Angle
1	1	121	0	0	0	121	33,8	0,2742	0,07759
1,5	1	121	0	0	0	121	35,7	0,0754	1,02185
2	1	85	0	0	0	85	37,6	0,0394	2,52739
2,5	1	89	0	0	0	89	39,5	0,0686	1,64416
3	1	85	0	0	0	85	41,4	0,1286	1,13806

In the first column of the table the frequency of each modulation is shown, in the second column it is shown k that is the number of steps that the modulation uses in the first quarter of a wave without counting the zero step, a, b, c and d define the vector L is only used in the table due to the low voltage level required for these frequencies, TC is the total number of switching angles, VRMS is the effective level obtained and THD is the total harmonic distortion of the modulation; as angles only three are shown, of the TC angles that exist in the modulation.

Figure 5 shows the graph of the control law 'Vvsf' established with the RMS values found by the algorithm

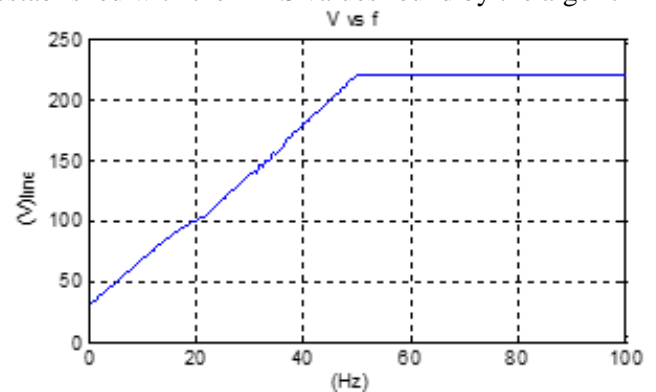


Fig. 5 Scalar relationship V/Hz according the Multiobjective algorithm.

Similarly, in Figure 6 shows the behavior of the total harmonic distortion with respect to frequency, the results show that in most frequencies is very close to 0%, however in the range of [40.5 42Hz] THD exceeds 1% and presents a maximum peak of 1.8%. In the same way these peaks comply fully with the requirement of 2% maximum

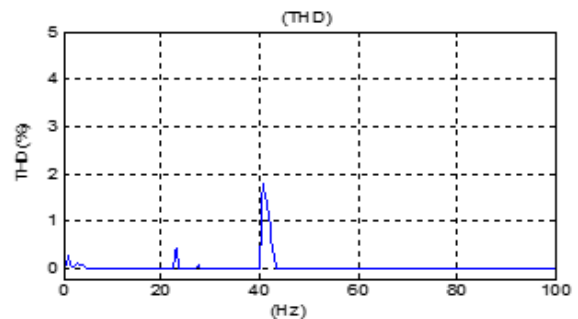


Fig. 6. Total harmonic distortion with respect to frequency.

In this way it is verified that the optimization algorithm is capable of generating a command law  $V_{vsf}$ , which guarantees a minimum of harmonic distortion at all operating frequencies.

### 5. Implementation

To validate the optimization carried out and the command law found, a multi-level inverter prototype of H bridges was implemented in cascade, with a common source with an asymmetric 1: 3 relationship and with the capacity to vary its frequency from 1 Hz to 100 Hz, the design of the transformers was carried out following the methodology proposed by the authors of this work [25].

To measure the total harmonic distortion and the line  $V_{rms}$  were used: the Fluke 125 oscilloscope and the Fluke 434 network analyzer. The network analyzer allows to measure the harmonic content of voltages and currents in the frequency range close to 50 or 60 Hz, however, for this application is not very useful, since it was intended to validate the frequencies between 1 and 100 Hz. The oscilloscope allows to measure the harmonic content of any frequency, however it will not have the same analyzer accuracy. Figure 6 shows the assembly of the test



Fig. 6 Assembly of the test

The results of the validation are given below, in the first part the waveforms and the harmonic spectrum given by the oscilloscope for several sample frequencies are shown. The THD shown is quite low, however it is not close to zero percent, this is due to the presence of the transformers and the lack of precision of the FFT of the oscilloscope, for this reason in the second part the validation is done with the analyzer Fluke 434 at frequencies close to 50 and 60 Hz.

Validation of control law  $V$  vs  $F$  and THD optimization  
The inverter presented an excellent behavior regarding the variation of the RMS value of the line voltage, in figure 7.a. The waveform of the voltage is observed at a frequency of 100 Hz (maximum frequency) and where the

RMS level is 220 Volts. The optimized harmonic spectrum of this voltage is shown in Figure 7. b.

The THD of the line voltage is 2.7%, being less than the 5% limit [29]. In figure 8.a. the waveform of the line voltage is observed at a frequency of 60 Hz which is a frequency above the rated and where the RMS voltage level is 220 Volts.

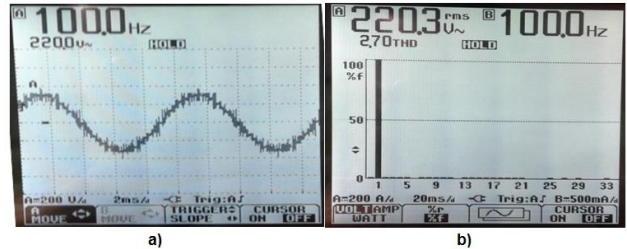


Figure.7 a) Line voltage waveform at 100 Hz  
b) Harmonic spectrum.

The Figure 8 b shows the optimized harmonic spectrum of the line voltage, whose THD is 2.6%, this complies fully with the 5% limit for low voltage systems [29]. The waveform is identical to the one in figure 7, this is due to the fact that modulations with frequencies higher than 50 Hz are the same because they have the same RMS value, only the pulse duration changes and therefore the frequency.

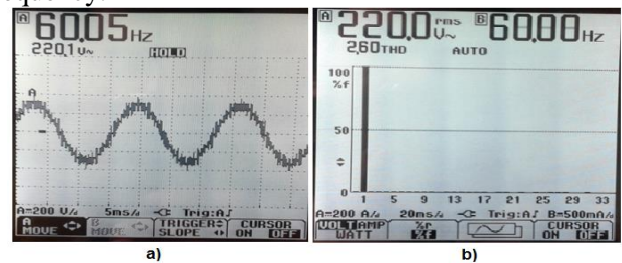


Figure. 8 a) Line voltage waveform at 60 Hz  
b) Harmonic spectrum

In figure 9.a. the waveform of the line voltage is observed at a frequency of 40 Hz and where the RMS voltage level is 156.9 Volts. As you can see, the waveform is different from the previous ones, this is due to the fact that the voltage level is lower, since the frequency is below the rated frequency.

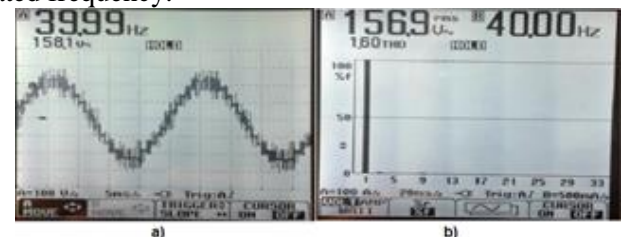


Figure. 9. a) Line voltage waveform at 40 Hz  
b) Harmonic spectrum.

The THD of the line voltage is 1.6%, this value is lower than that measured in the previous tests, this is because as the frequency drops, the measuring instrument can take more samples and make a more accurate calculation. The harmonic spectrum can be seen in figure 9.b where the optimization is evidenced.

In figure 10 .a. the waveform of the line voltage is observed at a frequency of 20 Hz, the RMS voltage level is 93.4 Volts. As you can see, the waveform has a lower number of steps than the previous ones, the number of levels is only 7, while in the line voltage shown in figure 9 it was 13 and in figures 7 and 8 it was 15 steps. The THD of the line voltage is 1.9%

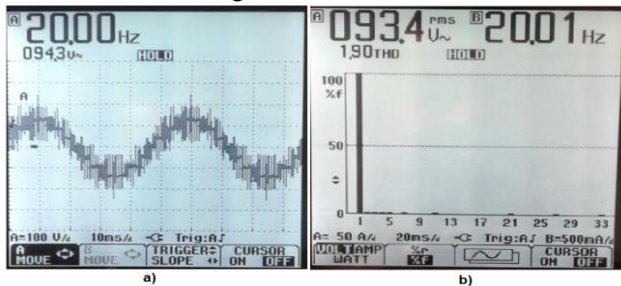


Fig.10 a) Line voltage waveform at 20 Hz  
b) Harmonic spectrum.

**Validation of the inverter's power quality**

In the following test the frequency inverter was placed to operate at 60 Hz and the line and phase voltages waveforms were captured to more accurately validate the harmonic content, the power quality and the operation of the inverter, for this the fluke 434 analyzer was used, figure 11 shows the comparison between the three phase voltage waveforms measured by the analyzer, Fluke 434

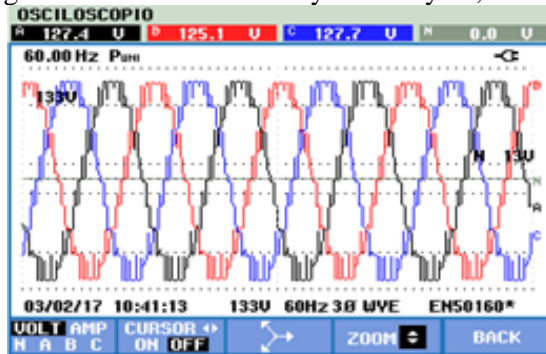


Fig 11. Three-phase voltage waveform

With respect to phase shifts, the following figure shows the phasor diagram of the three phase voltages measured by the Fluke analyzer.

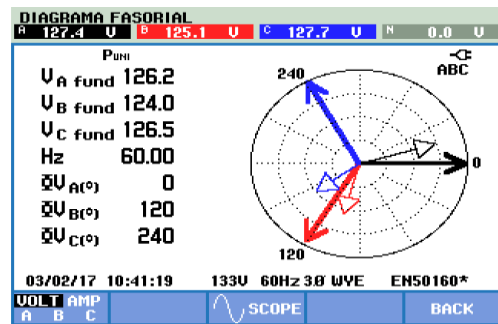


Fig 12. Phasor diagram of the three phase voltages.

Figure 13 shows the harmonic spectrum of the phase voltage where it shows that the harmonics present are the multiple of three 3, 9, 15, 21, 33 and 45, where the harmonic 33 has the greatest magnitude. As for the total of harmonic distortion in the observed that the THD is 10.9%. These harmonics disappear in line voltages, allowing the harmonic content of these voltages to be zero

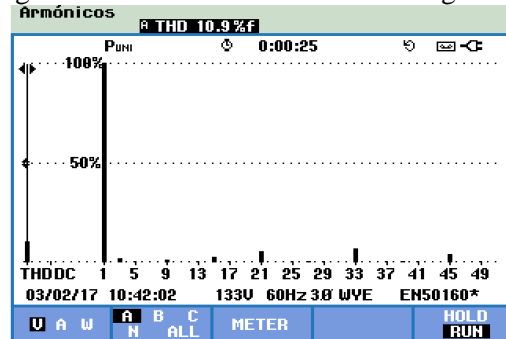


Fig. 13. Harmonic spectrum of the phase voltage

Figure 14 shows the line voltage waveforms measured by the oscilloscope, where it is observed that in the three lines the behavior is the same.

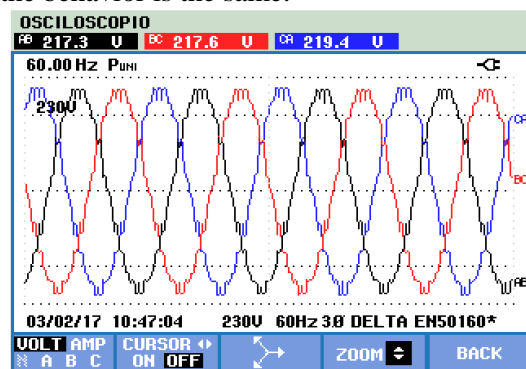


Fig 14. Three-phase voltage waveform

The effective values of the line voltages measured by the analyzer are shown in Table 2.

Table 2. Line voltage RMS values

Vrms líne AB	Vrms líne BC	Vrms líne CA
217.3 V	217.6 V	219.4 V

The line voltage RMS values are unbalanced due to the small imperfections in the construction of the phase

transformers, the unbalance between the line voltages is less than the unbalance between the phase voltages, presenting a value of 0.34%.

Figure 15 shows the phasor diagram measured in the operation of the frequency inverter connected to an induction motor of 450 W in order to observe the characteristics of the current.

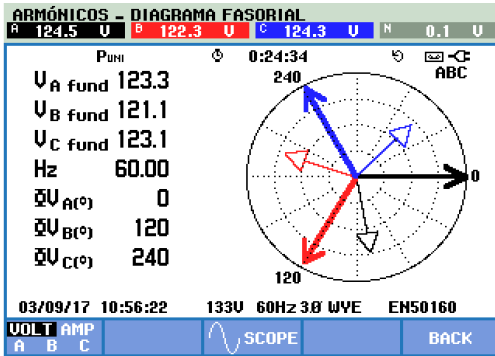


Fig. 15. Phasor diagram of the three phase voltages.

This figure shows that the phase differences of the system, of ABC positive sequence, is of 0, 120 and 240 electrical degrees, in the same way, it shows the lags of the currents that enter the motor, and it is clearly observed that the system is balanced.

Figure 16 shows the harmonic spectrum of the line voltage obtained in the experiment.

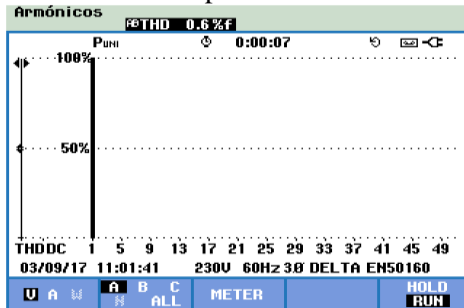


Fig. 16. Harmonic spectrum of the line voltage.

The given harmonic spectrum confirms the optimization performed by the inverter that adopts the modulation found by the optimization algorithm. The THD is 0.6% higher than that found by the optimization algorithm; due to the small disturbances exerted by the transformers used by the inverter. Figure 17 shows the spectrum of the three line voltages, it shows that the behavior is identical in the three voltages.

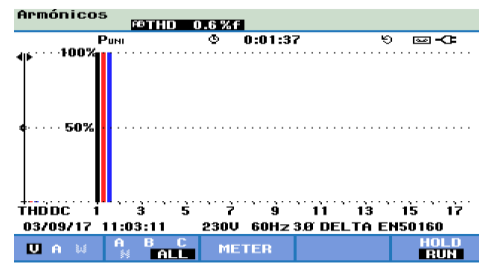


Fig. 17. Harmonic spectrum of the three line voltages.

Figure 18 shows the waveform of the stator currents of the motor, where you can see a virtually sinusoidal waveform in all three phases

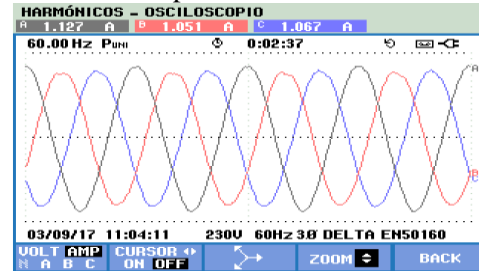


Fig.18 Waveforms of the three line currents.

Figure 19 shows the spectrum obtained in the test. It is observed that there is a presence of low order harmonics 2, 3, 4 and 5 due to the current waveform that the motor demands. However the THD is 2.3% a considerably low value

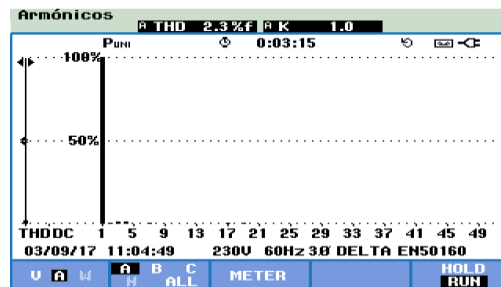


Fig. 19 Harmonic spectrum of the line current

Figure 20 shows the spectrum of the three line currents, it shows that the behavior is identical in all three phases

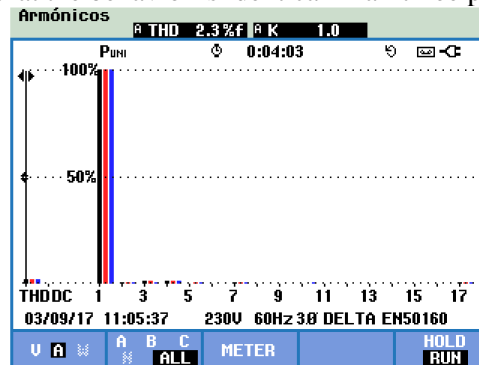


Fig. 20. Harmonic spectrum of the three line currents.

## 6. Conclusions

Within the review of the state of the art it was found that few works have been able to reduce the THD of the output voltage of a multilevel inverter below 1%, which is why this project gives an important contribution, having a wide range of modulations that theoretically have a harmonic content in line voltage less than 1% THD.

The THD measured experimentally for the line voltages shows the good functionality of the optimization algorithm performed, since in all the tests the THD is below 3%, the lowest value measured was 0.6% and the highest value of 3%, which are very low magnitudes for the Total Harmonic Distortion.

The command law  $V$  vs  $F$  found in that work, allows to vary the frequency from 1Hz to 100Hz, changing proportionally the voltage as the frequency decreases from its rated value, according to equation 13, however the algorithm can take any form of equation that involves  $V$  and  $F$ .

Because the optimization proposed in this work is done directly in the line voltage, the multiple of three harmonics can exist in the phases, since these are eliminated when realizing the potential difference between them, therefore in the line voltages there will be no , this is demonstrated in the mathematical modeling developed

The results regarding the THD of the line voltage, reflects the good design of the inverter, since it reproduces the waveforms calculated in an appropriate way. Although the inverter uses transformers at the output of the H bridges, the design thereof minimizes the disturbances that they can generate, that is why the THD is low even though they are used as variable frequency transformers. It is noteworthy that the bridge inverter H in common source cascade can indeed be used in variable frequency applications as long as the transformers are designed properly.

The feeding of the induction motor with multilevel power inverter and optimization of harmonics developed this work, offers advantages for the induction motor, such as the reduction of the harmonic components of the current and voltage, which theoretically decreases the ripple in the torque electromagnetic, in the speed and own currents, in this way problems like opposing pairs, overheating and other inconveniences associated with harmonic distortion are avoided.

The magnitude of the THDi depends on the frequency and the filtering performed by the inductances of the motor and the transformers. Despite this in all tests the

magnitude is below 5% and the contributions of each of the harmonics is very low

### References:

- [1] S. J. Chapman, Máquinas eléctricas, 5 ed., McGraw-Hill Interamericana, 2012.
- [2] A. E. Fitzgerald, C. Kingsley and S. D. Umans, Electric Machinery, Sexta edición ed., McGraw Hill, 2003.
- [3] P. Vas, Sensorless Vector and Direct Torque Control, Oxford: Clarendon Press, 1998.
- [4] T. H. Dos Santos, A. Goedel, d. S. S. A. Oliveira and M. Suetake, "Scalar control of an induction motor using a neural sensorless technique," Electric Power Systems Research, vol. 108, pp. 322-330, 2014.
- [5] M. A. Sanchez, Calidad de la energía eléctrica, Instituto Tecnológico de Puebla: Mexico, 2009.
- [6] Y. Mehmet, V. Seydi and V. y. H. C. Seci, "Comparison of Output Current Harmonics of Voltage Source Inverter used Different PWM Control Techniques," WSEAS transactions on power systems, pp. 696-703, 2008.
- [7] G. Barbera, H. G. Mayer and F. Issouribehere, "Medición de la emisión armónica en variadores de velocidad y desarrollo de modelos de simulación," in Encuentro Regional Iberoamericano de CIGRE 2009., 2009.
- [8] L. D. Pabón fernández, J. L. Diaz Rodríguez and A. E. Arevalo, "Multilevel power converter with variable frequency and low constant total harmonic distortion," in 2014 IEEE 5th Colombian Workshop on Circuits and Systems (CWCAS),, Bogotá, 2014.
- [9] M. Malinowski, K. Gopakumar, J. Rodriguez and M. Pérez, " A Survey on Cascaded Multilevel Inverters," IEEE Trans. on Ind. Elect., , vol. 57, no. 7, pp. 2197-2206, 2010.
- [10] J. Kavali and A. Mittal, "Analysis of various control schemes for minimal Total HarmonicDistortion in cascaded H-bridge multilevel inverter," Journal of Electrical Systems and Information Technology, 2016.
- [11] J. L. Diaz Rodríguez, J. L. Pabon Fernandez and A. Pardo Gracia, "THD Improvement of a PWM Cascade Multilevel Power Inverters Using Genetic Algorithms as Optimization Method", WSEAS Transactions On Power Systems, 2015.
- [12] A. Moeed Amjad, Z. Salam and A. Majed Ahmed, "Application of differential evolution for cascaded multilevel VSI with harmonics elimination PWM

switching," *International Journal of Electrical Power & Energy Systems*, 2015.

[13] G. Nageswara, P. Rao, R. Sangameswara and K. Chandra, "Harmonic elimination of cascaded H-bridge multilevel inverter based active power filter controlled by intelligent techniques," *International Journal of Electrical Power & Energy Systems*, 2014.

[14] L. D. Pabon Fernandez, J. L. Diaz Rodríguez and A. Pardo Garcia, "Total harmonic distortion optimization of the line voltage in single source cascaded multilevel converter," *WSEAS Transactions On Systems*, vol. 15, pp. 199 - 209, 2016.

[15] L D Pabon, E A Caicedo, J L Diaz, A Pardo Garcia. Configurable converter for performance assessment of cascaded multilevel power converters. *WSEAS transactions on power systems*, E-ISSN: 2224-350X, Volume 11, 2016.

[16] HA Meza, JLM García, SS Mora. Estrategias de control mppt aplicadas en un convertidor dc/dc tipo boost para sistemas fotovoltaicos. *Revista Colombiana de Tecnologías de Avanzada*. ISSN: 1692-7257. 2018.

[17] T. SudhakarBabu, K. Priya, D. Maheswaran, K. SathishKumar and N. Rajasekar, "Selective voltage harmonic elimination in PWM inverter using bacterial foraging algorithm," *Swarm and Evolutionary Computation*, p. 74–81, 2015.

[18] A. Chitra and S. Himavathi, "Reduced switch multilevel inverter for performance enhancement of induction motor drive with intelligent rotor resistance estimator," *IET Power Electronics*, p. 2444–2453, 2015.

[19] N. Jigar, Y. Mistry and H. Pratik, "Flying Clamped Capacitor Multilevel Inverter In Variable Frequency Drive," *International Journal of Advanced Research in Computer and Communication Engineering*, vol. 2, 2013.

[20] R. Taleba, D. Benyoucefa, M. Helaimia and Z. Boudje, "Cascaded H-bridge Asymmetrical Seven-level Inverter Using THIPWM for High Power Induction Motor," *Energy Procedia*, p. 844 – 853, 2015.

[21] R. Shriwastava, M. B. Daigavaneb and P. M. Daigavanec, "Simulation Analysis of Three Level Diode Clamped Multilevel Inverter Fed PMSM Drive Using Carrier Based Space Vector Pulse Width Modulation (CB-SVPWM)," *Procedia Computer Science*, p. 616 – 623, 2016.

[22] O Suarez, C Vega, E Sánchez, A González, O Rodríguez, A Pardo. Degradación anormal de p53 e inducción de apoptosis en la red p53-mdm2 usando la estrategia de control tipo pin. *Revista Colombiana de Tecnologías de Avanzada*. ISSN: 1692-7257, 2018.

[23] s. Manasa, "Design and simulation of three phase five level and seven level inverter fed induction motor drive with two cascaded h-bridge configuration," *international journal of electrical and electronics engineering*, p. 2231 – 5284, 2012.

[24] L. D. Pabón Fernández, J. L. Díaz Rodríguez and A. Pardo García, "Simulación del inversor multinivel de fuente común como variador de frecuencia para motores de inducción", *Revista De Investigación, Desarrollo E Innovación*, vol. 7, no. 1, pp. 1-10, 2016.

[25] A. Antonopoulos, G. Mörée, J. Soulard, L. Ängquist and H. Nee, "Experimental Evaluation of the Impact of Harmonics on Induction Motors Fed by Modular Multilevel Converters," in *Electrical Machines (ICEM)*, Berlin, 2014.

[26] A. K. Panda and Y. Suresh, "Research on cascade multilevel inverter with single DC source by using three-phase transformers," *International Journal of Electrical Power & Energy Systems*, pp. 9-20, 2012.

[27] J. L. Diaz-Rodríguez, L. D. Pabón-Fernández and E. A. Caicedo-Peñaranda, "Novel methodology for the calculation of transformers in power multilevel converters," *Ingeniería y competitividad*, 2015.

[28] A Araque, JLD Rodríguez, AS Guerrero. Optimización por recocido simulado de un convertidor multinivel monofásico con modulación pwm sinusoidal de múltiple portadora. *Revista Colombiana de Tecnologías de Avanzada*. ISSN: 1692-7257, 2017.

[29] IEEE, "IEEE Std. 519-1992 IEEE Recommended Practices and Requirements for Harmonic Control in Electrical Power Systems," IEEE, 1992.

[30] D. Goldberg, "Genetic Algorithms in Search, Optimization and Machine Learning". Addison-Wesley Publishing Company, 1989.

[31] R López, MG Angarita. AT Espinosa. Convertidores fotovoltaicos en módulos integrados basados en inversores de fuente-semi-cuasi-z: un nuevo esquema de control por modos deslisanes. *Revista Colombiana de Tecnologías de Avanzada*. ISSN: 1692-7257, 2014.